RSC Advances

PAPER

View Article Online
View Journal | View Issue

Cite this: *RSC Adv.*, 2021, **11**, 13047

Light-up photoluminescence sensing of a nerve agent simulant by a bis-porphyrin–salen–UO_2 complex†

Chiara Maria Antonietta Gangemi,[a] Ugne Rimkaite,[b] Andrea Pappalardo *[ac] and Giuseppe Trusso Sfrazzetto [ac]

Received 20th February 2021
Accepted 21st March 2021

DOI: 10.1039/d1ra01397a

rsc.li/rsc-advances

A luminescent bis-porphyrin–salen–UO_2 complex, showing a significant fluorescence light-up response upon reacting with **DMMP** (a simulant of nerve agents), is reported. The fluorescence change of this complex by excitation at 365 nm can be clearly observed with the naked eye, and this complex was successfully employed to construct a test paper to detect nerve agents.

In the last decades, the terroristic attacks and world conflicts have seen increasing use of unconventional weapons, leading to mass destruction.[1] The substances used are generally indicated as CBRN (chemical, biological, radiological, and nuclear) weapons. Among these, chemical warfare agents (CWAs) are organophosphate compounds that irreversibly bind and inhibit the enzyme acetylcholinesterase (AChE), thus preventing the message transfer mechanism of the nervous system, causing permanent health damages or death.[2] These nerve agents can easily aerosolise and vaporise when mixed with water and most other solvents and are mainly introduced in the human body through respiration and absorption by skin or eyes.

The nerve agents are classified into two main groups: "G-series" (the oldest early 1900 and non-persistent) and V-series (more recent 1950s and persistent), although very recently, the "A-series or Novichok agents", a new class of nerve agents, unfortunately deadlier than the previous series, has been developed. Hence, it is urgent to develop fast, easy, and highly sensing systems to detect in real time the presence of nerve agents, even at very low concentrations.[3] In fact, the toxicity of the common nerve agents is in the range of ppm or sub-ppm (LC_{50} values are 2 and 1.2 ppm for tabun and sarin, respectively, and even more low for soman and VX with LC_{50} values of 0.9 and 0.3 ppm).[4] Certainly, for safety reasons, CWAs cannot be used in common research laboratories. Thus, other substances, similar to the nerve agent for geometry and functional groups but less reactive, since they do not contain a good leaving group as observed in real warfare agents (*e.g.*, F and CN), are used as simulants. In this context, dimethyl methylphosphonate (**DMMP**) has been recognized as one of the best simulants for G series nerve agents (Chart 1).[5]

In the last few years, several methods, including chemical sensors based on silicon nanoribbon field-effect transistors (SiNR-FETs),[6] surface acoustic wave (SAW) devices,[7] coordination complexes containing ligands,[8] chemiresistive sensors,[9] mesoporous silica material containing BODIPY derivatives,[10] and gas chromatography-mass spectrometry, for the detection of CWAs have been developed.[11] More recently, two different methods for sensing CWAs and correlated simulants have been reported: (i) the covalent approach and (ii) a supramolecular approach. The former one is based on the reaction of the analyte with the sensor, leading to a measurable response (*i.e.*, fluorescence emission and UV-Vis absorption).[12] This approach has few drawbacks, such as single detection for each sensor (sensors cannot be reused) and the low selectivity of the sensors due to false-positive responses.[13] On the other hand, in the supramolecular approach, CWAs are recognised *via* non-covalent reversible interactions,[14] involving different recognition sites (multi-topic) and allowing the reuse of sensors after the interaction with simulants.[15]

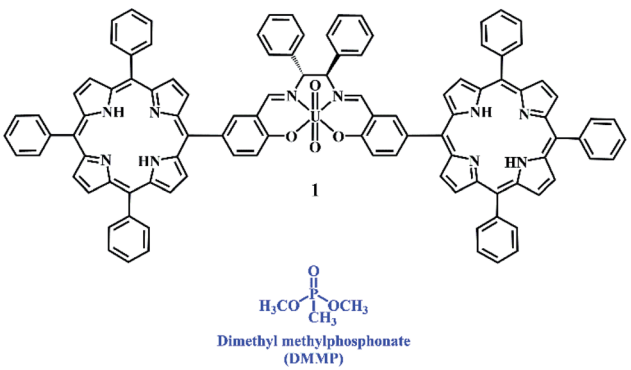

Chart 1 Chemical structures of bis-porphyrin–salen–UO_2 complex **1** and **DMMP**.

[a]*Department of Chemical Sciences, University of Catania, Viale Andrea Doria 6, 95125, Catania, Italy. E-mail: andrea.pappalardo@unict.it*

[b]*Faculty of Chemistry and Geosciences, University of Vilnius, Vilnius, Lithuania*

[c]*INSTM Udr of Catania, Viale Andrea Doria 6, 95125, Catania, Italy*

† Electronic supplementary information (ESI) available: Synthetic procedure and spectroscopic measurements. See DOI: 10.1039/d1ra01397a

During the last few years, metal–salen complexes have been used as hosts for the supramolecular detection of nerve gases. Atwood *et al.* reported an aluminium–salen complex for the detection of sarin and soman in an aqueous solution *via* ESI-MS experiments.[16] Very recently, we were able to detect the **DMMP** simulant using uranyl or zinc metal–salen complexes *via* UV-Vis and/or luminescence spectroscopy techniques, exploiting a Lewis acid–base interaction between the metal centre and the phosphate group of the simulant.[17] Unfortunately, many of these systems have shown a turn-off of fluorescence after interaction with the simulant. In fact, fluorogenic sensors represent a powerful tool for detecting CWAs because of the advantages of low cost, high sensitivity, and a real-time response.[18]

In order to overcome this problem, we have designed and synthesized a new luminescent bis-porphyrin–salen–UO_2 complex **1**, which is able to coordinate through uranyl ions to the P=O group of **DMMP**,[19] showing a fluorescence light-up response upon reacting with different concentrations of the simulant (Chart 1). In our strategy, the logical association of porphyrin derivatives, with their high stability and fluorescence properties, and uranyl–salen ligands, would lead to fluorogenic sensors that exhibit novel luminescence properties, which up to now were ruled out in uranyl–salen complexes due to the presence of uranyl metal ions. Moreover, complex **1** has been employed to construct a paper test for the naked-eye detection of **DMMP**. The targeted complex **1** was synthesized in three steps according to the sequence illustrated in Scheme 1.

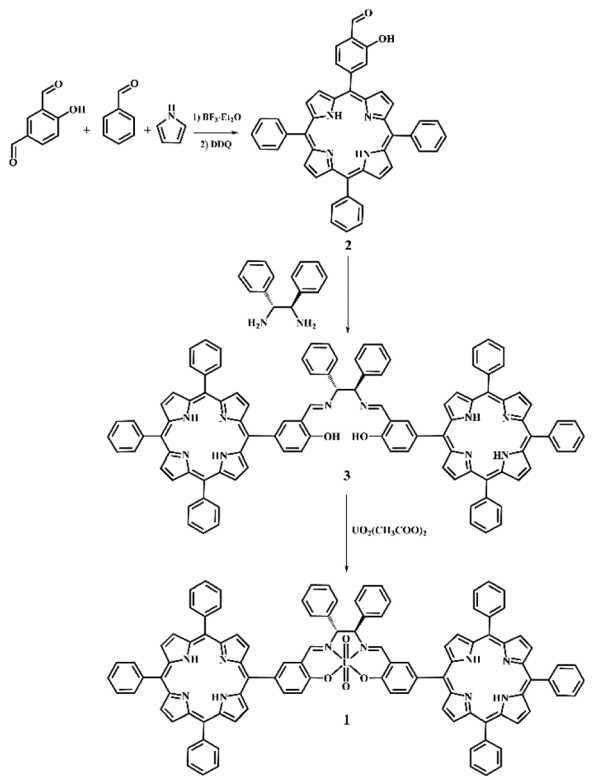

Scheme 1 Synthesis of bis-porphyrin–salen–UO_2 complex **1**.

The salicylic-porphyrin **2** was prepared by a statistical mixed-aldehyde condensation reaction according to the modified Lindsey procedure.[20] To a solution of benzaldehyde and pyrrole in $CHCl_3$, 4-hydroxyisophthalaldehyde was added in the presence of $BF_3 \cdot Et_2O$ as a catalyst. The obtained porphyrinogen was then oxidized using 2,3-dichloro-5,6-dicyanobenzoquinone (DDQ). The salicylic-porphyrin **2** was condensed with (1*R*,2*R*)-(+)-1,2-diphenylethylenediamine according to a classical literature procedure for salen synthesis,[21] affording the bis-porphyrin–salen ligand **3**, which was finally converted in the bis-porphyrin–salen–UO_2 complex **1** by uranyl acetate (overall yield 5.2%; see the ESI†).

With this complex in hand, we examined the detection performance towards **DMMP**. The spectroscopic characterization of complex **1** was conducted in $CHCl_3$. Fig. 1 shows the absorption and emission spectra of complex **1**.

In particular, the UV-Vis spectrum shows the Soret band at 422 nm ($\varepsilon = 3.1 \times 10^5$ M^{-1} cm^{-1}) and four Q-bands at 518 nm, 555 nm, 592 nm, and 650 nm, respectively. After excitation at 422 nm, two strong emission bands can be observed at 655 and 725 nm, relative to the $\pi \leftarrow \pi^*$ transition of the porphyrin core, in accordance with literature data for similar porphyrins.[20b] Φ_F yield (Φ = 0.51) was estimated using *N*-butyl-4-butylamino-1,8-naphthalimide as the standard ($\Phi_F = 0.81$).[22]

The sensing of **DMMP** was studied *via* fluorescence titrations in $CHCl_3$. The emission spectrum of **1** upon reacting with increasing amounts of **DMMP** showed a significant increase in the fluorescence signals at 625 nm and 725 nm (Fig. 2).

Job's plot supports the 1 : 1 stoichiometry of the host–guest complex (see the ESI†); thus, the binding constant value of log 6.54 ± 0.05 was calculated *via* a non-linear best fit,[23] monitoring the emission intensity at 655 nm and 725 nm, confirming the ability of sensor **1** to act as a light-up fluorescence host towards **DMMP**. According to LOD = $3\sigma/\kappa$, the detection limit of complex **1** for **DMMP** was 7.23 ppb, which is much lower with respect to the lethal doses of the most common CWAs. Thus, the high binding constant value, the low LOD, and the high Stokes shift (>233 nm) represent ideal features for a practical sensor.

To probe the selectivity of complex **1** towards **DMMP**, complex **1** was treated with numerous analytes, observing the change in the emission band. Complex **1** showed high

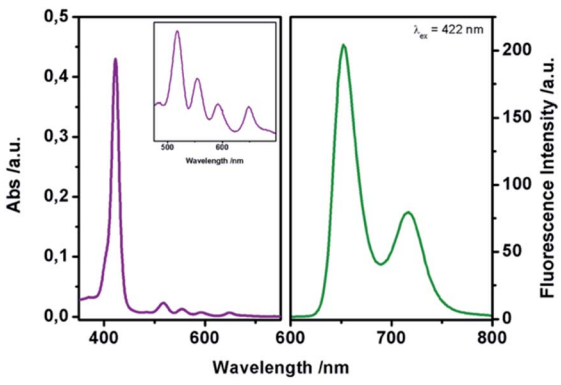

Fig. 1 Absorption (left) and emission (right, λ_{ex} = 422 nm) spectra of complex **1** in $CHCl_3$ 1 μM.

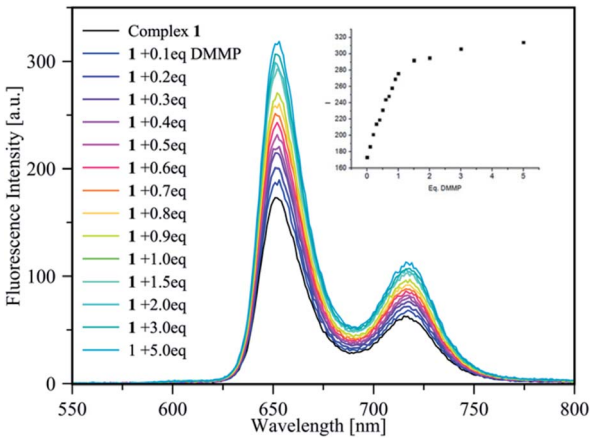

Fig. 2 Fluorescence titration of complex **1** (1 μM in $CHCl_3$) with increasing amount of DMMP (0–5 eq.); the inset shows the intensity increase upon the progressive addition of DMMP equivalents.

selectivity towards **DMMP** over interferent substances, including air (real conditions, containing 24 000 ppm water, 400 ppm CO_2, 5 ppm NO, and 10 ppm CO), triethylphosphine, triphenylphosphine, and acetone (see the ESI†). In addition, to verify the sensing properties of complex **1** also under competing conditions, to this solution, 1 eq. of **DMMP** has been added, leading to a significant increase in emission, thus showing hardly any interference with **DMMP** detection in the coexistence of **DMMP** and various analytes (Fig. 3).

Prompted by the highly attractive features of complex **1**, we used complex **1** as the main component to create a portable test paper for CWA detection. Thus, 45 μL of a 10 μM solution of **1** in CH_2Cl_2 was deposited onto the supports (filtration paper, 1.5 × 1.5 cm), and the solvent was removed. The supports were introduced into vials (23 mL of volume) containing different amounts of pure **DMMP**, and these systems were kept at 60 °C in order to vaporize the simulant. The **DMMP** vapours,

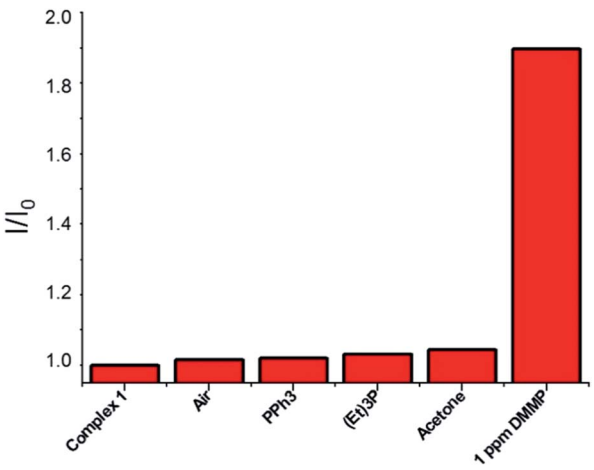

Fig. 3 Selectivity tests: normalized fluorescence responses of complex **1** (1×10^{-6} M in chloroform, λ_{ex} 422 nm) towards air (bubbled for 5 min), PPh_3 (2 ppm), $(Et)_3P$ (2 ppm), acetone (2 ppm), and DMMP (1 ppm). Analytes are sequentially added up to the final addition of DMMP. Bars represent the final (I) over the initial (I_0) emission intensity at 625 nm.

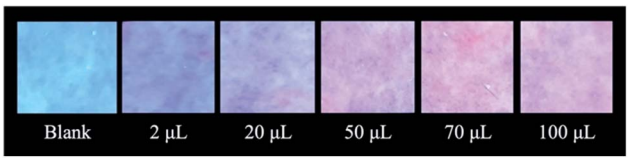

Fig. 4 Qualitative tests of complex **1** absorbed onto the filtration paper and exposed to an increasing amount of DMMP vapours (2 μL, 20 μL, 50 μL, 70 μL, 100 μL, at 60 °C).

interacting with the uranyl-complex *via* Lewis acid–base interactions, induced an increment in the fluorescence of complex **1** adsorbed on the paper upon excitation at 365 nm, which is more evident in the presence of a higher quantity of **DMMP** vapours, leading to significant colour changes from light blue to purple (Fig. 4). Moreover, complex **1** absorbed onto the filtration paper and was exposed to selected oxygenated molecules (*e.g.*, acetone, ethanol, and Et_2O) did not show colour changes (see the ESI†).

Moreover, the system was found to be reversible. In fact, after exposure to air for 24 h at 60 °C, the device returns to the original condition without differences in terms of fluorescence with respect to the unused device, consequently confirming the non-covalent nature of the interactions between the sensor and the guest. Finally, the reusability of the device was tested for five cycles of absorption/desorption of **DMMP** without any loss in efficiency (Fig. 5).

These results indicate that the strategy we planned has led to the development of a simple test paper for the rapid detection of nerve agents.

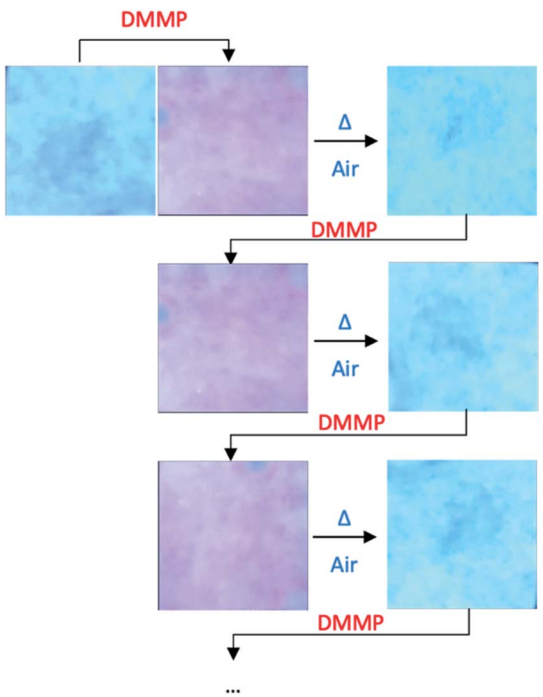

Fig. 5 Colour changes of complex **1** onto the paper support during cyclic DMMP detection/reactivation processes.

In summary, the new fluorescent sensor reported here shows a strong light-up response in the presence of the CWA simulant, with a high binding constant value and low limit of detection (ppb level), much lower with respect to the lethal dose of the most common CWAs. The presence of the porphyrin units is crucial for obtaining these emission properties. In addition, the paper tests confirmed the possibility of using this sensor for real applications due to the possibility to monitor the presence of a low concentration of CWAs also in the gas phase. The supramolecular approach allows restoring and reusing the initial device. Currently, we are working to obtain a quantitative detection of the simulant in gas phase by image elaboration.

Conflicts of interest

There are no conflicts to declare.

Notes and references

1 (*a*) D. Dons, *Science*, 2013, **341**, 1051; (*b*) D. Butler, *Nature*, 2018, **556**, 285–286.
2 G. Mercey, T. Verdelet, J. Renou, M. Kliachina, R. Baati, F. Nachon, L. Jean and P.-Y. Renard, *Acc. Chem. Res.*, 2012, **45**, 756–766.
3 (*a*) S. Royo, R. Martinez-Manez, F. Sancenon, A. M. Costero, M. Parrab and S. Gil, *Chem. Commun.*, 2007, 4839–4847; (*b*) D. Ajami and J. Rebek Jr, *Org. Biomol. Chem.*, 2013, **11**, 3936–3942.
4 S. W. Wiener and R. S. Hoffman, *J. Intensive Care Med.*, 2004, **19**, 22–37.
5 J. Lavoie, S. Srinivasan and R. Nagarajan, *J. Hazard. Mater.*, 2011, **194**, 85–91.
6 S. Clavaguera, A. Carella, L. Caillier, C. Celle, J. Pécaut, S. Lenfant, D. Vuillaume and J.-P. Simonato, *Angew. Chem., Int. Ed.*, 2010, **49**, 4063–4066.
7 J. Kim, H. Park, J. Kim, B.-I. Seo and J.-H. Kim, *Sensors*, 2020, **20**, 7028.
8 L. Ordronneau, A. Carella, M. Pohanka and J.-P. Simonato, *Chem. Commun.*, 2013, **49**, 8946–8948.
9 J. F. Fennell Jr, H. Hamaguchi, B. Yoon and T. M. Swager, *Sensors*, 2017, **17**, 982.
10 E. Climent, M. Biyikal, K. Gawlitza, T. Dropa, M. Urban, A. M. Costero, R. Martinez-Manez and K. Rurack, *Sens. Actuators, B*, 2017, **246**, 1056–1065.
11 H. Nagashima, T. Kondo, T. Nagoya, T. Ikeda, N. Kurimata, S. Unoke and Y. Seto, *J. Chromatogr. A*, 2015, **1406**, 279–290.
12 X. Zhou, S. Lee, Z. Xu and J. Yoon, *Chem. Rev.*, 2015, **115**, 7944–8000.
13 Y. J. Jang, K. Kim, O. G. Tsay, D. A. Atwood and D. G. Churchill, *Chem. Rev.*, 2015, **115**, PR1–PR76.
14 (*a*) M. R. Sambrook and S. Notman, *Chem. Soc. Rev.*, 2013, **42**, 9251–9267; (*b*) G. Trusso Sfrazzetto, S. Millesi, A. Pappalardo, G. A. Tomaselli, F. Ballistreri, R. M. Toscano, I. Fragalà and A. Gulino, *Chem.–Eur. J.*, 2017, **23**, 1576–1583; (*c*) R. Puglisi, P. G. Mineo, A. Pappalardo, A. Gulino and G. Trusso Sfrazzetto, *Molecules*, 2019, **24**, 2160.
15 (*a*) N. Tuccitto, L. Riela, A. Zammataro, L. Spitaleri, G. Li-Destri, G. Sfuncia, G. Nicotra, A. Pappalardo, G. Capizzi and G. Trusso Sfrazzetto, *ACS Appl. Nano Mater.*, 2020, **3**, 8182–8191; (*b*) R. Puglisi, A. Pappalardo, A. Gulino and G. Trusso Sfrazzetto, *ACS Omega*, 2019, **4**, 7550–7555.
16 R. R. Butala, W. R. Creasy, F. A. Roderick, M. L. McKee and D. A. Atwood, *Chem. Commun.*, 2015, **51**, 9269–9271.
17 (*a*) R. Puglisi, A. Pappalardo, A. Gulino and G. Trusso Sfrazzetto, *Chem. Commun.*, 2018, **54**, 11156–11159; (*b*) L. Legnani, R. Puglisi, A. Pappalardo, M. A. Chiacchio and G. Trusso Sfrazzetto, *Chem. Commun.*, 2020, **56**, 539–542.
18 (*a*) W. Meng, Y. Chen, Y. Feng, H. Zhang, Q. Xu, M. Sun, W. Shi, J. Cen, J. Zhao and K. Xiao, *Org. Biomol. Chem.*, 2018, **16**, 6350–6357; (*b*) W. Meng, W. Shi, Y. Chen, H. Zhang, J. Zhao, Z. Li and K. Xiao, *Sens. Actuators, B*, 2018, **281**, 871–877; (*c*) W. Meng, M. Sun, Q. Xu, J. Cen, Y. Cao, Z. Li and K. Xiao, *ACS Sens.*, 2019, **4**, 2794–2801; (*d*) A. K. Yadav, C. J. Reinhardt, A. S. Arango, H. C. Huff, L. Dong, M. G. Malkowski, A. Das, E. Tajkhorshid and J. Chan, *Angew. Chem., Int. Ed.*, 2020, **59**, 3307–3314; (*e*) J. Zhang, X. Chai, X. P. He, H. J. Kim, J. Yoon and H. Tian, *Chem. Soc. Rev.*, 2019, **48**, 683–722.
19 (*a*) M. E. Amato, F. P. Ballistreri, A. Pappalardo, G. A. Tomaselli, R. M. Toscano and D. J. Williams, *Eur. J. Org. Chem.*, 2005, 3562–3570; (*b*) G. M. Lombardo, A. L. Thompson, F. P. Ballistreri, A. Pappalardo, G. Trusso Sfrazzetto, G. A. Tomaselli, R. M. Toscano and F. Punzo, *Dalton Trans.*, 2012, **41**, 1951–1960; (*c*) G. Brancatelli, A. Pappalardo, G. Trusso Sfrazzetto, A. Notti and S. Geremia, *Inorg. Chim. Acta*, 2013, **396**, 25–29.
20 (*a*) J. S. Lindsey, I. C. Schreiman, H. C. Hsu, P. C. Kearney and A. M. Marguerettaz, *J. Org. Chem.*, 1987, **52**, 827–836; (*b*) C. M. A. Gangemi, U. Rimkaite, F. Cipria, G. Trusso Sfrazzetto and A. Pappalardo, *Front. Chem.*, 2019, **7**, 836.
21 (*a*) F. P. Ballistreri, A. Pappalardo, G. A. Tomaselli, R. M. Toscano and G. Trusso Sfrazzetto, *Eur. J. Org. Chem.*, 2010, 3806–3810; (*b*) M. E. Amato, F. P. Ballistreri, S. D'Agata, A. Pappalardo, G. A. Tomaselli, R. M. Toscano and G. Trusso Sfrazzetto, *Eur. J. Org. Chem.*, 2011, 5674–5680; (*c*) A. Pappalardo, M. E. Amato, F. P. Ballistreri, G. A. Tomaselli, R. M. Toscano and G. Trusso Sfrazzetto, *J. Org. Chem.*, 2012, **77**, 7684–7687.
22 X. Guo, X. Qian and L. Jia, *J. Am. Chem. Soc.*, 2004, **126**, 2272–2273.
23 (*a*) A. Pappalardo, F. P. Ballistreri, G. Li Destri, P. G. Mineo, G. A. Tomaselli, R. M. Toscano and G. Trusso Sfrazzetto, *Macromolecules*, 2012, **45**, 7549–7556; (*b*) R. Puglisi, F. P. Ballistreri, C. M. A. Gangemi, R. M. Toscano, G. A. Tomaselli, A. Pappalardo and G. Trusso Sfrazzetto, *New J. Chem.*, 2017, **41**, 911–915.